Coupling of a Turbulent Flow and Surface Recession

X. Lamboley[a,b], G.L. Vignoles[a], J. Mathiaud[b,c], J. Couzi[b], B. Dubroca[a,b], T.-H. Nguyen-Bui[b,c]

a. Laboratoire des Composites ThermoStructuraux, UMR 5801
3 allée de la Boétie, 33600 Pessac
b. CEA/CESTA, 15 Avenue des Sablières, 33114 Le Barp
c. Centre Lasers Intenses et Applications (CELIA), UMR 5107
43 rue Pierre Noailles, 33400 Talence

Résumé

Lors de la phase de retour dans l'atmosphère, un corps de rentrée va subir de très fortes températures (> 2000 K) et pressions (> 100 bar) à sa surface. C'est pourquoi des protections thermiques composées de composites carbone/carbone sont utilisées. À sa surface vont avoir lieu de nombreux phénomènes parmi lesquels des réactions hétérogènes entre le carbone et l'environnement (oxidation, nitruration), et à de plus hautes températures, la sublimation. Cette activité chimique va provoquer le recul de la paroi du bouclier thermique. L'écoulement autour de l'objet évolue d'un régime laminaire au régime turbulent, associés à une rugosité de la surface caractéristique. Le régime laminaire est caractérisé par une rugosité microscopique [Levet(2017)], qui va alors favoriser localement la transition laminaire-turbulent. Apparaissent alors des structures macroscopiques (de l'ordre du centimètre). Enfin, l'écoulement devient pleinement turbulent, menant au développement de structures de plus petite échelle [Hochrein et Wright Jr(1976)], cette fois-ci généralisées à toute la surface. On les appelle "scallops" (parfois "coups de gouge" en français), et peuvent augmenter drastiquement les transferts de chaleur et les vitesses de récession de la paroi [Wool(1975)], c'est pourquoi l'étude de leur formation et évolution est fondamentale pour la conception des protections thermiques.

Abstract

*During an atmospheric reentry, the heat shield protecting the body will undergo very high temperature (> 2000 K) and pressure (> 100 bar) on its surface. This is why thermal protection systems (TPS) are used, composed especially of **3D carbon/carbon composites**. Numerous phenomena will occur on the surface, in particular heterogeneous chemical reactions between the carbon and the surrounding air (oxidation, nitridation) and, at higher temperatures, sublimation ; these reactions will cause the recession of the surface of the composite heat shield. All along the reentry phase, the flow around the body will evolve, with in each regime characteristic surface roughness features caused by the ablation of the composite material. The laminar flow is associated with a microscopic roughness dimension [Levet(2017)], due to the material manufacturing history. Then the slight ondulations of the material will favour the **transition to turbulence** on located spots on the surface, and will give birth to macroscopic patterns with a centimetre scale . The flow will finally become **fully turbulent**, with the development of a new type of patterns of a millimetre scale [Hochrein et Wright Jr(1976)], no more localised this time but generalised to the whole surface. These characteristic patterns are known as **"scallops"**. They are able to*

multiply the heat transfer and the recession rate by more than 2 [Wool(1975)] ; therefore understanding their formation and behaviour is a necessity for a better design of TPS.

Mots clefs : ablation ; turbulence ; surface patterns ; carbon/carbon composite ; incompressible flow

1 Introduction

The flow above a recessive surface sees the development of characteristic patterns on the material, different according to the regime of the flow. Indeed, the surface recession, caused by the heterogeneous reaction of the solid material with the surrounding air, is not uniform on the surface ; it is in close relation with the turbulence regime of the flow (Fig. 1). These typical surface ondulations may also occur on different types of interactions and different scales, such as melting in ice caverns, sublimation in the case of meteorites or sediment transport by air or water for sand dunes for example (Fig. 2, [Leighly(1948)], [Anderson Jr et al.(1998)]).

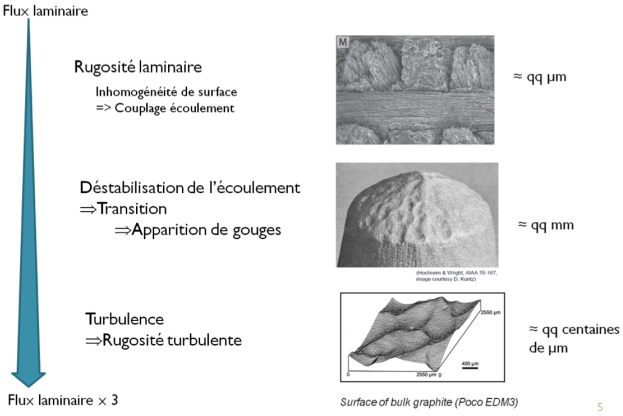

FIGURE 1 – Surface rougness types according to the flow regime

About reentry bodies, the laminar flow will firstly lead to the development of a microscopic roughness, due in particular to the weaving of the carbon/carbon composite and the reactivity contrast between the matrix and the fibres [Levet(2017)]. Then, this microscopic surface roughness will favour the transition of the flow to the turbulence on located spots of the surface.

This transitional regime, which is the main study of this paper, is characterised by a strong increase of the mass and heat flux [Schneider(2006)]. It will lead to the development of macroscopic and regular ondulations, known as "scallops".

Finally, the flow will reach the fully turbulent regime, where the patterns shape will decrease in size and return to a millimetre roughness.

It is proposed here to determine a scenario for the development of these scallops, and a numerical simulation using the open-source code OpenFoam of the surface instabilities along the development of turbulence.

(a) Ice caverns

(b) Dunes

(c) "Cabin Creek" meteorite

FIGURE 2

2 Problem definition and simulation setup

2.1 Case setup and mesh

The reentry flows of interest are typically hypersonic, and can reach Mach 20 on some applications. However for the study of the interaction of the turbulence and the surface recession, the simulation domain is located inside the Mach cone backwards the shock wave, and an incompressible simulation is considered.

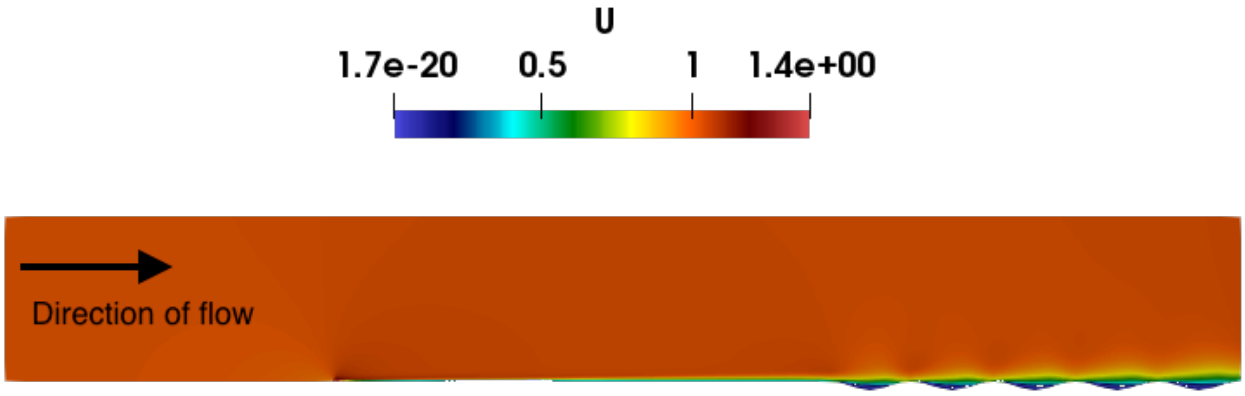

FIGURE 3 – 2D simulation domain

The 2D simulation domain is then the fluid above a flat plate, including the stagnation point. In order to trigger the instability, the surface is given an initial ondulation, once the turbulent boundary layer is established. Since no wall functions are used, the mesh at the wall must be really fine, respecting the criterion $y^+ < 1$. The resolution is computed with OpenFoam [Weller et al.(1998)], using the algorithm *SIMPLE* for steady flows, and *PIMPLE* for unsteady ones.

2.2 Governing equations

2.2.1 RANS equations

We consider a reacting fluid flow over a bed. Following the classic Reynolds averaging description, one obtains the incompressible RANS equations (Reynolds Averaged Navier-Stokes), with ρ the fluid density, U_i are the components of the mean velocity and p the mean pressure :

$$\begin{aligned} \partial_j U_j &= 0 \\ \rho \partial_t U_i + U_j \partial_j U_i &= \partial_j \tau_{ij} - \partial_i p, \end{aligned}$$

where the stress tensor τ_{ij} containing the Reynolds stress depends on the kinematic viscosity ν :

$$\tau_{ij} = \rho\nu \left(\partial_i U_j + \partial_j U_i - \frac{2}{3} \nabla . \mathbf{U} \delta_{ij} \right) - \rho \overline{U_i' U_j'},$$

Considering a reacting flow, a reactant (either oxygen or nitrogen) is considered and has the molar concentration C. Thanks to the conservation of the oxydant mass, it obeys the following convection-diffusion equation containing the diffusion coefficient D and the turbulent mass fluxes $\overline{U_j' C'}$:

$$\partial_t C + U_j \partial_j C = D \partial_j C + \overline{U_j' C'}$$

2.2.2 Turbulence modeling

This RANS approach requires a turbulent closure, i.e. the modelling of turbulent stresses and turbulent mass fluxes. For that purpose, turbulence is considered to add viscosity in the flow, and the turbulent stresses are modelled with a turbulent viscosity ν_t, following the Boussinesq hypothesis :

$$\overline{U_i' U_j'} = \nu_t \left(\partial_i U_j + \partial_j U_i\right)$$

In the same way, turbulent mass fluxes are calculated with a turbulent diffusion coefficient D_t.

$$\overline{U_j' C'} = D_t \partial_j C$$

The turbulent diffusion coefficient is usually taken proportional to the turbulent viscosity : $D_t = \dfrac{\nu_t}{Sc_t}$, and a typical value for the turbulent Schmidt number Sc_t is 0.7 [Gualtieri et al.(2017)].
The $k-\omega$ SST 2-equation turbulence model was chosen in OpenFoam [Menter(1993)], for its suitability in flat plate simulations. This model uses transport equations for the turbulence kinetic energy k and the specific rate of dissipation ω. The turbulent viscosity is then $\nu_t = \frac{k}{\omega}$.
However, this model is not able to reproduce correctly the by-pass transition to turbulence, in particular the increase in wall shear stress in the transitional zone. That is why an extension to this model was used, the 4-equation model $\gamma - Re_\theta$ [Langtry(2006)]. This solves two additional equations for the rate of turbulence γ and the transition momentum thickness Reynolds number Re_θ.
Because an accurate description of the turbulence on the wall is of primary importance here, no wall laws are used. The boundary conditions for k and ω must be provided with the classical values [Menter(1993)] :

$$\begin{aligned} k_{wall} &= 0 \\ \omega_{wall} &= \frac{60\nu}{0.075\ \delta y^2} \end{aligned}$$

2.2.3 Surface reactivity and recession

The oxydant transported in the flow will also react with the surface material. A first order heterogeneous reaction is considered, leading to the mixed boundary condition on the bed :

$$\left(D + D_t\right) \nabla C = k_r C$$

with k_r the surface reactivity which depends on the temperature of the surface. It is to be noted that the total diffusion coefficient is used here, reflecting the fact that the turbulence brings an additional flux of oxydant on the surface.
Finally, the surface itself will recess vertically under the action of the chemical reaction. If Z is the height of the surface, the recession velocity in function of the molar volume of the solid υ_s and the surface reactivity is given with the Hamilton-Jacobi equation

$$\partial_t Z = -\upsilon_s k_r C$$

2.3 Microscopic roughness modelling

As stated already, the transition from laminar to turbulent occurs once a laminar roughness of microscopic dimension has been developed. To account for that, a sand-grain equivalent roughness model is used [Nikuradse(1937)]. Following the work of [Knopp et al.(2009)], the roughness height k_s will modify the boundary conditions of k and ω at the wall ; in particular, $\nu_t = \dfrac{k}{\omega}$ does not vanish. It depends on the adimensioned roughness height k_s^+ :

$$\begin{aligned} k_s^+ &= \frac{k_s u_*}{\nu}, \quad u_* = \sqrt{\frac{|\tau_{xz}|}{\rho}}, \quad \tau_w = (\nu + \nu_t)\, \partial_y U|_{y=0} \\ k_{wall} &= \phi_{r1} k_{rough}, \quad k_{rough} = \frac{u_*^2}{\sqrt{\beta_k}} \\ \omega_{wall} &= min\left(\frac{u_*}{\sqrt{\beta_k}\kappa \tilde{d}_0}, \frac{60\nu}{0.075\ \delta y^2}\right), \quad \tilde{d}_0 = \phi_{r2} 0.03 k_s \end{aligned}$$

where $\phi_{r1}(k_s^+)$ and $\phi_{r2}(k_s^+)$ are blending functions and $\beta_k = 0.09$ is a constant in the $k-\omega$ model. It is noted that $\dfrac{k_{wall}}{\omega_{wall}} = \nu_{t,wall}$ depends only on k_s^+, which means that surface roughness changes the viscosity on the surface independently of the local shear stress.

3 RANS simulations results

3.1 Highlighting the laminar to turbulent transition

The phenomenon of "scalloping" has been evidenced from experiments [Hochrein et Wright Jr(1976)] to rely on the transition from laminar to turbulent. Numerical experiments on a flat plate where carried out, comparing the $k-\omega SST$ and $\gamma - Re_\theta$ models (Fig. 4). The velocity at the upstream is U_∞ and the length of the domain is L.

It shows that near the stagnation point the flow remains laminar ; then from a given distance around $Re_x = \dfrac{U_\infty x}{\nu}$ the skin friction will rapidly increase. After that, the turbulence in the boundary layer is fully developed. The transition point will come closer to the stagnation point as $Re = \dfrac{U_\infty L}{\nu}$ increases.

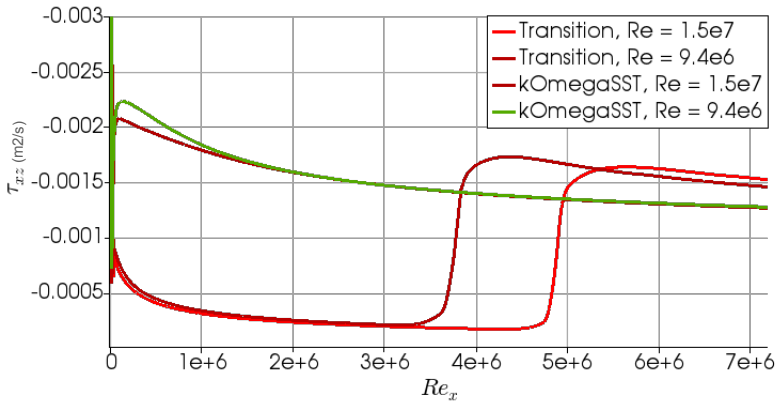

FIGURE 4 – Shear stress τ_{xz} along Re_x over a flat plate

The sudden increase of friction at the wall will cause the increase of diffusion of oxydant. This mechanism creates localised "spots" of oxydant at the wall, giving birth to crests on the surface of the

material.

3.2 Wall shear stress distribution above an ondulated surface

Once a first trough have been initiated, it is investigated now the stability of system, i.e. wether an initial surface instability will grow or decrease. For that purpose, the simulation domain is extended with ondulations once the fully developed boundary layer has been attained, with the frequency $\frac{2\pi}{k}$ and the amplitude h.

Showing the maximum skin friction before ondulations against $\frac{k\nu}{u_*}$ (Fig. 5), it is noted a local maximum around 10^{-3}, which corresponds to a transitional flow. This is in close agreement with [Thomas(1979)] which compiled experiments of naturally-formed ripples in different conditions and showed this correlation $\lambda = 10^{-3}\frac{\nu}{u_*}$.
[Claudin et al.(2017)] also gets this result with a linear stability analysis of the boundary layer equations.

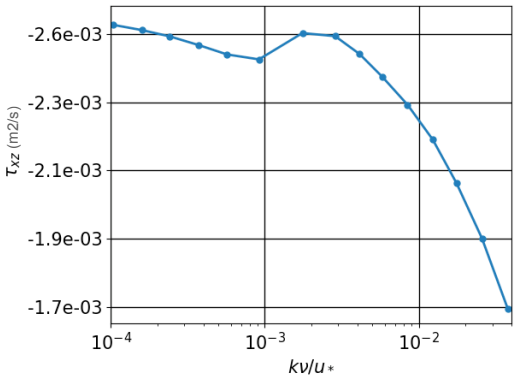

FIGURE 5 – τ_{xz} versus $\frac{k\nu}{u_*}$ before ondulations once the fully developed boundary layer is developed

Further on the plate, the ripple creates variations in the wall shear stress and thus in the surface concentration (Fig. 6). For any set of parameters, a maximum appears just before the top of the ondulation. Moreover for a transitional flow, a recirculation appears downstream, creating a positive maximum in basal shear stress inside the hollow due to the relaminarisation of the flow. The concentration is also maximal inside the trough. The $k-\omega SST$ model is unable to capture this phenomenon as shown in figure 6, that is the reason why the $\gamma - Re_\theta$ model was used.

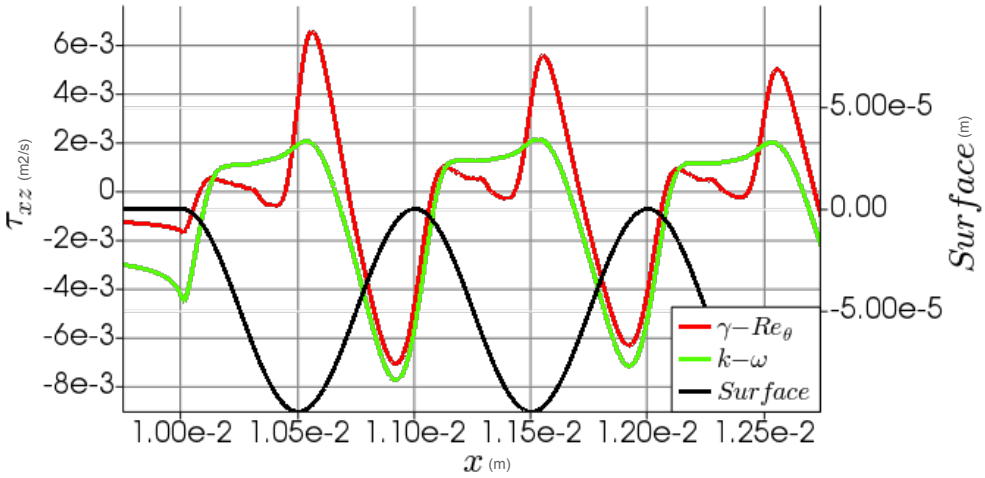

FIGURE 6 – Shear stress τ_{xz} along the horizontal coordinate x above an ondulated plate

However in our simulations, the maximum of concentration in the trough always stays lower than before the crest whatever the parameters $\frac{k\nu}{u_*}$ or kh ; this indicates that the initial ondulation will always decrease

in time. Additionally, increasing the microscopic surface roughness only results in dampening the basal shear stress not playing a major role in the surface stability.

3.3 Morphology evolution

The phase of these extrema which depends on our two parameters, will involve the morphology evolution (Fig. 7) ; indeed, if the oxydant concentration is in phase with the surface, this means that more material will be consumed on the crests and less in the troughs, leading to the damping of the surface. In the reverse, the phase opposition would amplify the surface ondulations. A dephasing of $\frac{\pi}{2}$ correspond to a maximum before a crest, causing a forward transport of the ondulation, and $-\frac{\pi}{2}$ would be a backwards transport.

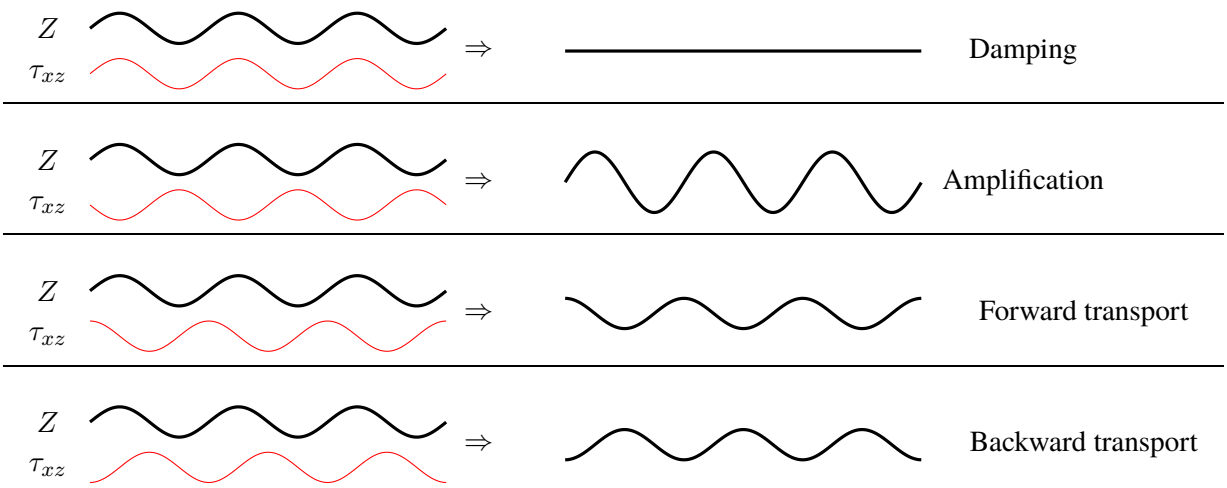

FIGURE 7 – Surface evolution depending on the phase of the basal shear stress with the surface

The case presented above correspond to a superposition of the three first situations : the oxydant concentration presents extrema both before the crest and in the trough, and the global maximum is the one before the crest. This would lead to a forward transport of the surface ondulations, slowly dampened due to the maximum in the trough.

4 Conclusion

The characteristic pattern formation appearing when coupling a reacting flow with an erodible surface is due to the local variations of basal shear stress. It occurs at the laminar-turbulent transition, which sees a sudden increase of friction and oxydant concentration on the plate around $Re_x = 4\ 10^6$. Once this initial surface perturbation created, the oxydant concentration greatly increases in the trough due to the relaminarisation of the flow in this region ; this mechanism will maintain the disruption. The turbulence model of [Langtry(2006)] was required in order to capture correctly the relaminarisation downstream of the crest.

Although the flux remains always greater before the crest than in the trough, the surface will be transported while slowly dampened over time, due to the phase of the surface with the surface concentration. Future work includes the study of other geometries which might be able to create a bigger recirculation, leading to an amplification of the initial disruption. Ablation involves much more phenomena than oxydation, such as sublimation or pyrolysis, which may be taken into account in future studies.

Références

[Anderson Jr et al.(1998)] Anderson Jr, C. H., C. J. Behrens, G. A. Floyd, M. R. Vining, C. H. J. Anderson, C. J. Behrens, G. A. Floyd, et M. R. Vining, 1998, Crater firn caves of Mount St Helens, Washington, *Journal of Cave and Karst Studies*, *60*, (1), 44–50, 1998.

[Claudin et al.(2017)] Claudin, P., O. Durán, et B. Andreotti, 2017, Dissolution instability and roughening transition, *Journal of Fluid Mechanics*, *832*, R2, 2017.

[Gualtieri et al.(2017)] Gualtieri, C., A. Angeloudis, F. Bombardelli, S. Jha, et T. Stoesser, 2017, On the Values for the Turbulent Schmidt Number in Environmental Flows, *Fluids*, *2*, (4), 17, 2017.

[Hochrein et Wright Jr(1976)] Hochrein, G. J., et G. F. Wright Jr, Analysis of the TATER Nosetip Boundary Layer Transition and Ablation Experiment, in *14th Aerospace Sciences Meeting*, number 76, 0–10, American Institute of Aeronautics and Astronautics, Reston, Virigina, jan 1976.

[Knopp et al.(2009)] Knopp, T., B. Eisfeld, et J. B. Calvo, 2009, A new extension for k-ω turbulence models to account for wall roughness, *International Journal of Heat and Fluid Flow*, *30*, (1), 54–65, 2009.

[Langtry(2006)] Langtry, R. B., 2006, A Correlation-Based Transition Model using Local Variables for Unstructured Parallelized CFD codes, *Journal of Turbomachinery*, 2006.

[Leighly(1948)] Leighly, J., 1948, Cuspate Surfaces of Melting Ice and Firn, *Geographical Review*, *38*, (2), 300–306, 1948.

[Levet(2017)] Levet, C., *Ablation de matériaux carbonés sous très haut flux : étude multi-physique de l'interaction avec l'écoulement*, Ph.D. thesis, Université de Bordeaux, apr 2017.

[Menter(1993)] Menter, F. R., 1993, Zonal Two Equation k-omega Turbulence Models for Aerodynamic Flows, *AIAA Journal*, 1993.

[Nikuradse(1937)] Nikuradse, J., Laws of flows in rough pipes. Technical report, technical report, NACA, WA, 1937.

[Schneider(2006)] Schneider, S. P., 2006, Laminar-Turbulent Transition on Reentry Capsules and Planetary Probes, *Journal of Spacecraft and Rockets*, *43*, (6), 2006.

[Thomas(1979)] Thomas, R. M., 1979, Size of scallops and ripples formed by flowing water, *Nature*, *277*, 281–283, 1979.

[Weller et al.(1998)] Weller, H. G., G. Tabor, H. Jasak, et C. Fureby, 1998, A tensorial approach to computational continuum mechanics using object-oriented techniques, *Computers in Physics*, *12*, (6), 620, 1998.

[Wool(1975)] Wool, M., Passive Nosetip Technology (PANT) Program, Summary of Experimental and Analytical Results, technical report, 1975.